RSC Advances

PAPER

View Article Online
View Journal | View Issue

Cite this: *RSC Adv.*, 2020, **10**, 6464

Comparison of the oxidation of halogenated phenols in UV/PDS and UV/H_2O_2 advanced oxidation processes†

Junxin Liu, Yongze Liu, Yajun Tian, Li Feng* and Liqiu Zhang *

UV/peroxydisulfate (PDS) and UV/hydrogen peroxide (H_2O_2) can effectively degrade halophenols (HPs, *e.g.*, 2,4-bromophenol and 2,4,6-trichlorophenol); meanwhile, information about the discrepancies in the related degradation kinetics and mechanisms of these two processes is limited. To gain this knowledge, the degradation of two typical HPs (*i.e.*, bromophenols and chlorophenols) in UV/PDS and UV/H_2O_2 processes were investigated and compared. The results showed that the degradation rates of HPs with different substitution positions in the UV/PDS process were in the order of *para*-substituted HPs (*i.e.*, 4-BP and 4-CP) > *ortho*-substituted HPs (*i.e.*, 2-BP and 2-CP) > *meta*-substituted HPs (*i.e.*, 3-BP and 3-CP), while in the UV/H_2O_2 process, these rates were in the order of *para*-substituted HPs > *meta*-substituted HPs > *ortho*-substituted HPs. These discrepancies were ascribed to the different reaction activities of $SO_4^{\bullet-}$ and HO$^\bullet$ with HPs, which were calculated based on the competition method. Further density functional theory (DFT) calculations suggested that $SO_4^{\bullet-}$ reacts more readily with HPs *via* electron transfer than HO$^\bullet$. In the presence of water matrices (such as Cl^-, HCO_3^- and natural organic matter (NOM)), the degradation of 2-BP in both UV/PDS and UV/H_2O_2 treatment processes was inhibited due to the scavenging of free radicals by these background substances. The degradation products and pathways further confirmed that $SO_4^{\bullet-}$ is a strong one-electron oxidant that reacts with HPs mainly *via* electron transfer, while HO$^\bullet$ reacts with HPs *via* electron transfer and hydroxyl addition.

Received 11th December 2019
Accepted 22nd January 2020

DOI: 10.1039/c9ra10401a

rsc.li/rsc-advances

1. Introduction

Halogenated phenols (HPs) are typical halogenated compounds that have received increasing attention in recent years due to their potential hazards to water environments and human health.[1,2] Halogenated compounds have been widely used as brominated flame retardants, refrigerants, preservatives, *etc.*[3,4] With the high production and usage of halogenated compounds, large amounts of HPs (*e.g.*, bromophenols (BPs) and chlorophenols (CPs)) are released from those compounds and discharged into water environments.[5,6] HPs have been reported to be frequently detected in surface water environments at the ng L^{-1} to μg L^{-1} level.[7,8] The wide occurrence of HPs in water environments aggravates their environmental risk to ecosystems. Toxicological studies indicate that frequent exposure to HPs may result in injury to the skin, eyes and upper respiratory tract of humans to varying degrees.[9,10] Therefore, it is imperative to develop more effective technologies to remove these HPs from contaminated water environments.

Many HPs are recalcitrant contaminants, which are resistant to conventional biological and physico-chemical methods.[11–13] In recent years, UV-based advanced oxidation processes (AOPs) have been widely applied to degrade refractory organic pollutants through oxidizing agents such as H_2O_2.[14,15] The photolysis of H_2O_2 can generate hydroxyl radicals (HO$^\bullet$, redox potential 2.73 V).[16] Persistent organic pollutants (*e.g.*, phenol, azo dyes and some pharmaceuticals) were reported to be degraded in the UV/H_2O_2 process *via* HO$^\bullet$ oxidation.[17] The formed HO$^\bullet$ was demonstrated to have a fast reaction rate with HPs ($k = 10^8$ to 10^{10} M^{-1} s^{-1}).[18] Recently, the activation of peroxydisulfate (PDS) *via* UV photolysis has also been widely studied and applied in wastewater treatment.[19] The sulfate radical ($SO_4^{\bullet-}$) generated in the UV/PDS process was demonstrated to be a strong oxidative radical with a redox potential of 2.60 V.[16,20] Compared with HO$^\bullet$-based AOPs, $SO_4^{\bullet-}$ can react more rapidly with organic pollutants *via* electrophilic reactions.[21] $SO_4^{\bullet-}$-based AOPs have also been proved to have the ability to remove HPs with a removal rate of 80–100% after 30 minutes of reaction.[22] In a word, both HO$^\bullet$- and $SO_4^{\bullet-}$-based AOPs can degrade HPs effectively. However, in most literature reports focused on the degradation efficiencies of HPs in UV/PDS and UV/H_2O_2 processes, the discrepancies in HP degradation between UV/PDS and UV/H_2O_2 are not systematically researched. Furthermore, information about the degradation differences of HPs by the above two types

Beijing Key Laboratory for Source Control Technology of Water Pollution, Engineering Research Center for Water Pollution Source Control and Eco-remediation, Beijing Forestry University, Beijing 100083, China. E-mail: fengli_hit@163.com

† Electronic supplementary information (ESI) available. See DOI: 10.1039/c9ra10401a

of free radicals, especially the difference in the oxidized active sites of $HO^{\bullet}$ and $SO_4^{\bullet-}$, is limited.

In this study, to investigate the difference in the active sites of HPs between $HO^{\bullet}$ oxidation and $SO_4^{\bullet-}$ oxidation and to gain more thorough knowledge about the reaction mechanisms of $HO^{\bullet}$ and $SO_4^{\bullet-}$ oxidation, three bromophenols (BPs, 2-, 3-, and 4-BP) and three chlorophenols (CPs, 2-, 3-, and 4-CP) were selected as the target HPs. Firstly, the degradation kinetics of the HPs in UV/PDS and UV/H_2O_2 processes were comparatively examined; then, the active sites of the HPs were revealed based on density functional theory (DFT). In addition, the effects of the background matrix (such as pH, Cl^-, HCO_3^-, and NOM) on the degradation behaviors in UV/PDS and UV/H_2O_2 were evaluated. Furthermore, the degradation products and pathways of HPs in both processes were proposed.

2. Materials and methods

2.1. Chemicals

BPs (2-, 3-, and 4-BP, 98%) and CPs (2-, 3-, and 4-CP, 98%) were obtained from Macklin Biochemical Co. Ltd., (Shanghai, China). Potassium peroxodisulfate ($K_2S_2O_8$, 99%) and *tert*-butyl-alcohol (TBA, 99%) were obtained from Macklin Biochemical Co., LTD. (USA). H_2O_2 solution (35% w/w), sodium hydrogen carbonate ($NaHCO_3$, analytical grade), sodium chloride (NaCl, analytical grade) and potassium dihydrogen phosphate (KH_2PO_4, analytical grade) were acquired from Beijing Chemical Reagent Co. Ltd. (Beijing, China). Perchloric acid ($HClO_4$, 72%) and benzoic acid (BA, 99%) were obtained from Xilong Chemical Co., Ltd., China. Acetonitrile (99.9%) and methanol (99.9%) were of chromatographic grade (J.T. Baker Inc., USA). The standard NOM was acquired from the International Humic Substances Society (IHSS), where the NOM was extracted from the Suwannee River. The stock solution of NOM was obtained *via* stirring the solid in pure water for 48 h; then, the solution was centrifuged and the supernatant was filtered through 0.45 μm mixed cellulose ester membrane. The concentration of the total organic carbon (TOC) of the stock solution was measured with a TOC analyzer. The ultrapure water (>18.2 Ω m) used in this study was prepared using a water purification system (Cascada TM LS). All the chemical reagents used in the experiment were analytical grade or above.

2.2. Experimental procedures

The experiments were performed in a 100 mL cylindrical vessel reactor (diam. 50 mm) equipped with four low-pressure mercury ultraviolet (UV) lamps (GPH 212T5L/4, 10 W, Heraeus) emitting at 254 nm. The UV lamps were placed 30 cm above the cylindrical vessel reactor. The UV incident intensity (I_0, 253.7 nm) was determined to be 6.82×10^{-8} einstein per L per s *via* iodine–iodide spectrophotometry;[23] the optical path length of the reactor was 4 cm. The experimental solutions contained the target pollutant (10 μM) and PDS or H_2O_2 (0.5 mM). The pH value of the experimental solution was maintained at 7.0 with 10 mM phosphate buffer, and all experiments were performed at room temperature (25 ± 1 °C).

During the UV irradiation (30 min), 1.5 mL samples were withdrawn every five minutes (0, 5, 10, 15, 20, 25, 30 min). The samples were filtrated using 0.22 μm membranes (polyether sulfone, diam. 13 mm), and excess methanol was added to quench $SO_4^{\bullet-}$ and $HO^{\bullet}$. Then, the concentrations of the target contaminants were detected using high-performance liquid chromatography (HPLC). All of the experiments were carried out three times, and the results were averaged. All of the standard deviations were less than 5%.

In the competitive kinetics experiment, BA (10 μM) and HPs were added to the reaction system at the same time, and the second-order reaction rate constant was calculated by the competitive degradation kinetics during the UV/H_2O_2 process. TBA (10 mM) was added to the UV/PDS system to capture $HO^{\bullet}$ to create a single $SO_4^{\bullet-}$ system.

2-BP (pK_a = 8.45) was selected to further investigate the effects of pH and the background matrix (*i.e.*, Cl^-, HCO_3^- and NOM) on the HP degradation behavior in UV/PDS and UV/H_2O_2. The reaction solution pH was adjusted to different levels (*i.e.*, 4.0, 5.0, 6.0, 7.0 and 8.0) with perchloric acid and sodium hydroxide before irradiation to explore the effects of pH on the HP degradation. Specific volumes of stock Cl^-, HCO_3^- and NOM solutions were added to the reaction solution to obtain different concentrations of Cl^- (1, 5, 10, 100 and 500 mM), HCO_3^- (1 and 5 mM) and NOM (1, 5 and 10 mgC L^{-1}) to study the influence of the water matrices on the HP degradation.

In order to analyze the degradation products, the concentration of 2-BP was increased to 1 mM. Accordingly, the concentrations of PDS and H_2O_2 were also increased to 20 mM. The pH of the solutions was still maintained at 7.0. The samples (30 mL) were withdrawn after UV irradiation at 0, 15 and 30 min, respectively. Then, the samples were concentrated *via* solid-phase extraction and examined by liquid chromatography-tandem mass spectrometry (LC-MS/MS).

2.3. Analytical methods

The concentrations of BPs and CPs were determined using an HPLC (HPLC1260, Agilent, USA) equipped with a UV detector. A Poroshell 120 EC-C18 column (4.6 × 50 mm, 2.7 μm, Agilent, USA) was employed, and the column was maintained at 30 °C with a flow rate of 0.5 mL min^{-1}. The mobile phase consisted of water/acetonitrile (50 : 50, v/v%) for 2-BP, 2-CP, 3-BP and 3-CP and water/acetonitrile (45 : 55, v/v%) for 4-BP and 4-CP. All of the target compounds were detected at 280 nm. The concentration of NOM was analyzed by a TOC analyzer (Analytic Jena TOC-multiN/C 3100, Japan).

The degradation products of 2-BP were analyzed by liquid chromatography-tandem mass spectrometry (LC-MS/MS). Chromatography was performed using a Waters BEH C18 (1.7 μM × 100 mm) column. The details of the test method are provided in Text S2.†

2.4. Analytical methods

In order to compare the degradation mechanisms of HPs with different positions of substituted halogens in UV/PDS and UV/H_2O_2 treatment processes, the highest occupied molecular

orbitals and lowest occupied molecular orbitals (HOMO and LUMO) were calculated. Firstly, the geometries of the HPs were optimized with DFT based on B3LYP/6-311 (d,p) using Gaussian 09 software. Then, the HOMO/LUMO energies were further calculated with Multiwfn.[24]

3. Results and discussion

3.1. Degradation kinetics of BPs and CPs in the UV/PDS and UV/H_2O_2 processes

The degradation of different BPs and CPs in the UV/PDS and UV/H_2O_2 treatment processes followed first-order kinetics, as compared in Fig. 1a–d. In the UV/PDS process (Fig. 1a and c), the observed rate constants (*i.e.*, k_{obs}) of 2-BP, 3-BP, 4-BP, 2-CP, 3-CP, and 4-CP were calculated to be 0.0471 min^{-1}, 0.0282 min^{-1}, 0.0542 min^{-1}, 0.0345 min^{-1}, 0.0255 min^{-1} and 0.0386 min^{-1}, respectively. In the UV/H_2O_2 system (Fig. 1b and d), the k_{obs} of 2-BP, 3 BP, 4-BP, 2-CP, 3-CP, and 4-CP were calculated as 0.0301 min^{-1}, 0.0348 min^{-1}, 0.0379 min^{-1}, 0.0238 min^{-1}, 0.0330 min^{-1} and 0.0360 min^{-1}, respectively.

The HPs were degraded by direct photodegradation to a certain extent under UV irradiation (Fig. S1†); therefore, the observed rate constants (k_{obs}) for degradation of the HPs comprised those of direct photolysis (k_{UV}) and oxidation by radicals ($k_{radicals}$), as described in eqn (1).[25]

$$k_{obs} = S \times k_{UV} + k_{radicals} \quad (1)$$

where S is a screening correction considering the light filtering effect of the solution; the details of its calculation are shown in Text S1.† Thus, the direct UV photolysis rates of the HPs could be corrected *via* $S \times k_{UV}$ (the details of S are shown in Tables S1 to S3†); then, the rate of oxidation by radicals could be obtained, as shown in Tables S4 to S6.† In this section, the contributions of direct photolysis and oxidation by radicals are given in Fig. 1. It can be seen that direct photodegradation only contributed 8% to 15% to the HP degradation, and the HPs were mainly degraded *via* oxidation by radicals formed in the UV/PDS and UV/H_2O_2 processes.

It can be seen that the k_{obs} of the HPs with different substitution positions in UV/PDS were in the order of *para*-substituted HPs (*i.e.*, 4-BP and 4-CP) > *ortho*-substituted HPs (*i.e.*, 2-BP and 2-CP) > *meta*-substituted HPs (*i.e.*, 3-BP and 3-CP). The k_{obs} of the HPs in the UV/H_2O_2 process were in the order of *para*-substituted HPs (*i.e.*, 4-BP and 4-CP) > *meta*-substituted HPs (*i.e.*, 3-BP and 3-CP) > *ortho*-substituted HPs (*i.e.*, 2-BP and 2-CP), which is inconsistent with the order of the UV/PDS process.

In general, $SO_4^{\bullet-}$ is the main active radical in the UV/PDS process, while the main active specie in the UV/H_2O_2 process is $HO^{\bullet}$.[26] Thus, in order to further investigate the differences in the degradation of HPs with different substitution positions, the second-order reaction rate constants of the six target HPs with $SO_4^{\bullet-}$ and $HO^{\bullet}$ were calculated by competition kinetics. BA was employed to carry out the competition kinetics experiments

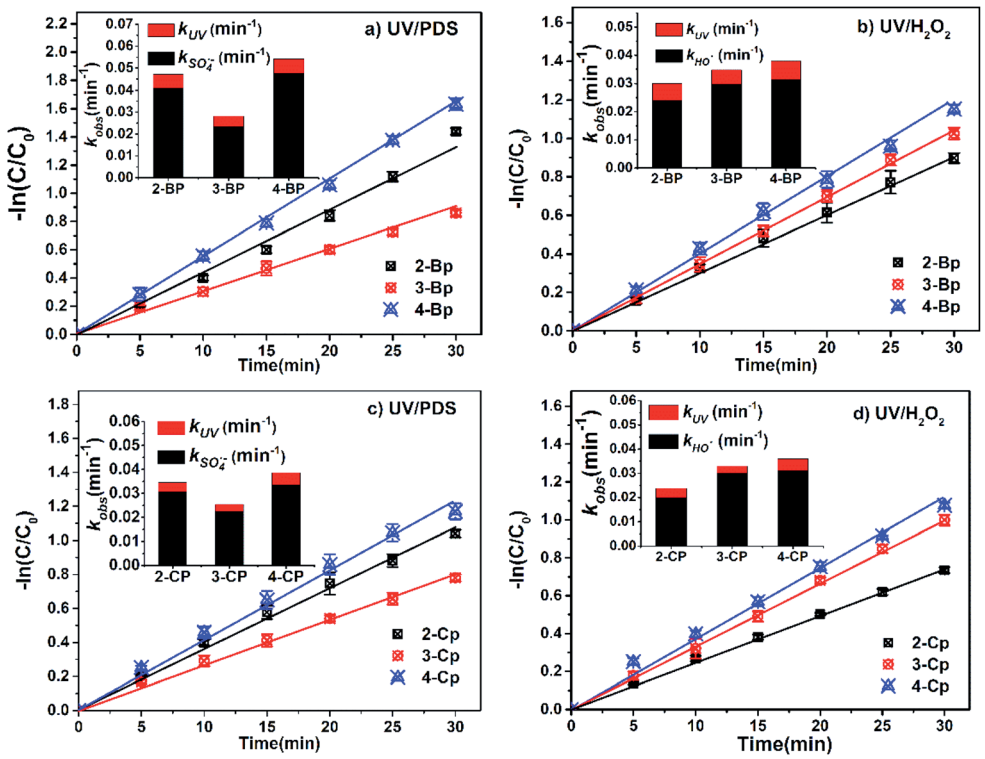

Fig. 1 The k_{obs} of degradation of BPs and CPs in UV/PDS and UV/H_2O_2 processes. (a) The k_{obs} of BPs degradation in UV/PDS process, (b) the k_{obs} of BPs degradation in UV/H_2O_2 process, (c) the k_{obs} of CPs degradation in UV/PDS process, (d) the k_{obs} of CPs degradation in UV/H_2O_2 process. Experimental conditions: [BPs] = [CPs] = 10 μM; 10 mM phosphate buffer (pH 7.0); [PDS] = [H_2O_2] = 0.5 mM.

due to its negligible photolysis under UV irradiation, and TBA was employed to quench HO$^{\bullet}$ in the UV/PDS process to obtain single $SO_4^{\bullet-}$ oxidation. The second-order reaction rate constants of BPs with $SO_4^{\bullet-}$ and HO$^{\bullet}$ were calculated *via* eqn (2) and (3); here, the second-order reaction rate constants of BA with $SO_4^{\bullet-}$ ($k_{SO_4^{\bullet-},BA}$) and HO$^{\bullet}$ ($k_{OH^{\bullet},BA}$) were reported to be 1.20 $\times$ 10^9 M^{-1} s^{-1} and 5.90 $\times$ 10^9 M^{-1} s^{-1}, respectively.[27]

$$\ln\frac{[BP]_0}{[BP]_t} - S \times k_{UV}t = \frac{k_{SO_4^{\bullet-},BP}}{k_{SO_4^{\bullet-},BA}}\ln\frac{[BA]_0}{[BA]_t} \quad (2)$$

$$\ln\frac{[BP]_0}{[BP]_t} - S \times k_{UV}t = \frac{k_{OH^{\bullet},BP}}{k_{OH^{\bullet},BA}}\ln\frac{[BA]_0}{[BA]_t} \quad (3)$$

The calculated second-order reaction rate constants of BPs and CPs with $SO_4^{\bullet-}$ and HO$^{\bullet}$ are given in Table 1. The $k_{SO_4^{\bullet-},BP}$ values were in the order of *para*-substituted HPs (*i.e.*, 4-BP and 4-CP) > *ortho*-substituted HPs (*i.e.*, 2-BP and 2-CP) > *meta*-substituted HPs (*i.e.*, 3-BP and 3-CP). The $k_{OH^{\bullet},HP}$ values were in the order of *para*-substituted HPs (*i.e.*, 4-BP and 4-CP) > *meta*-substituted HPs (*i.e.*, 3-BP and 3-CP) > *ortho*-substituted HPs (*i.e.*, 2-BP and 2-CP). Therefore, the different degradation rates of HPs with different substitution positions in the UV/PDS and UV/H_2O_2 processes can be attributed to their different reactivities with $SO_4^{\bullet-}$ and HO$^{\bullet}$.

Frontier orbital theory is usually used to explain the mechanisms of radical reactions.[28,29] In this study, quantum chemical calculations based on DFT were introduced to explain the differences in HP degradation between the UV/PDS and UV/H_2O_2 processes. According to the DFT calculations (Table 2), the HOMO energies of 2-BP, 3-BP, 4-BP, 2-CP, 3-CP, and 4-CP were determined to be −6.617243, −6.662641, −6.433939, −6.726734, −6.748275, and −6.577766 eV, respectively. The absolute values of the HOMO were in the order of 4-BP < 2-BP < 3-BP and 4-CP < 2-CP < 3-CP. Based on previous reports that a lower absolute value of the HOMO represents higher electrophilic reactivity,[30] these results suggest that the electrophilic reactivities are in the order of 4-BP < 2-BP < 3-BP and 4-CP < 2-CP < 3-CP. This indicates that electrophilic reactions are most likely to occur at the *para* halogen atom of the HPs due to its highest charge density (*i.e.*, lowest absolute value of the HOMO). It should be noted that the order of electrophilic reactivity was also consistent with that of the second order rate constants of $SO_4^{\bullet-}$ with the BPs/CPs, confirming that the reactions of the BPs/CPs with $SO_4^{\bullet-}$ mainly occur *via* electron transfer. However, in the case of HO$^{\bullet}$, the order of the second order rate constants of the BPs/CPs with HO$^{\bullet}$ were not all in agreement with that of the electrophilic reactivity of the BPs/CPs. This is because in addition to the electron transfer reaction, HO$^{\bullet}$ is prone to oxidize *via* H-abstraction and addition reactions.[21] In addition, it can be seen from Table 1 that the second-order reaction rate constants of the HPs and HO$^{\bullet}$ were greater than those of the HPs with $SO_4^{\bullet-}$. This is likely due to the faster H-abstraction reaction of HO$^{\bullet}$ than of $SO_4^{\bullet-}$. It has been reported that the H-abstraction reaction of HO$^{\bullet}$ is 1 to 2 orders of magnitude faster than that of $SO_4^{\bullet-}$.[21]

Table 1 Second-order reaction rate constants of six HPs with $SO_4^{\bullet-}$ and HO$^{\bullet}$

Compound	$SO_4^{\bullet-}$ (M^{-1} s^{-1})	HO$^{\bullet}$ (M^{-1} s^{-1})
2-BP	2.74×10^9	3.93×10^9
3-BP	2.70×10^9	5.81×10^9
4-BP	3.84×10^9	5.94×10^9
2-CP	2.58×10^9	4.19×10^9
3-CP	2.16×10^9	5.01×10^9
4-CP	3.37×10^9	6.84×10^9

Table 2 HOMO and LUMO orbital energies of the six HPs

Compound	HOMO energy (eV)	LUMO energy (eV)
2-BP	−6.617243	−0.722943
3-BP	−6.662641	−0.750628
4-BP	−6.433939	−0.839727
2-CP	−6.726734	−0.758318
3-CP	−6.748275	−0.788026
4-CP	−6.577766	−0.843039

3.2. Effects of pH on the degradation of 2-BP

As shown in Fig. 2, with increasing pH from 4.0 to 8.0, the k_{obs} of 2-BP in both the UV/PDS and UV/H_2O_2 processes decreased firstly from pH 4.0 to 5.0 and then increased from pH 6.0 to 8.0. The degradation efficiencies of 2-BP in both processes were the highest at pH 8.0.

This is because as the pH value of the solution increased (6.0 to 8.0), the deprotonation specie of 2-BP (pK_a = 8.45) was enhanced, and the ionic 2-BP was more readily oxidized, resulting in the increase of k_{obs}.[18] In addition, as shown in Fig. 2, the direct photolysis of 2-BP is weak under acidic and neutral conditions; meanwhile, it is significant under alkaline conditions because the dissociated phenolate is more electron-rich when formed at higher pH values. When the pH decreased from 6.0 to 4.0, the k_{obs} of 2-BP increased gradually; this is mainly due to the increased yields of the two free radicals with increasing acidity of the solution.[31]

In addition, phosphate buffer was employed to control the pH in these experiments; the concentration of HPO_4^{2-} in the buffer increased gradually while the concentration of $H_2PO_4^-$ decreased with increasing pH, and the ability of HPO_4^{2-} to capture free radicals was higher than that of $H_2PO_4^-$ (*i.e.*, k'' of HPO_4^{2-} with $SO_4^{\bullet-}$ and HO$^{\bullet}$, $H_2PO_4^-$ with $SO_4^{\bullet-}$ and HO$^{\bullet}$: 1.2 $\times$ 10^6 M^{-1} s^{-1}, 1.5 $\times$ 10^5 M^{-1} s^{-1}, 7.2 $\times$ 10^4 M^{-1} s^{-1} and 2.0 $\times$ 10^4 M^{-1} s^{-1}, respectively (eqn (4) to (7))).[27] Therefore, the change of the pH value may change some ion concentrations (*e.g.*, HPO_4^{2-} and HPO_4^-) and influence the steady-state concentrations of free radicals, which further impacts the degradation of HPs in the UV/PDS and UV/H_2O_2 processes.

$$SO_4^{\bullet-} + H_2PO_4^- \rightarrow \text{products}, k = 7.2 \times 10^4\ M^{-1}\ s^{-1} \quad (4)$$

$$SO_4^{\bullet-} + HPO_4^{2-} \rightarrow SO_4^{2-} + HPO_4^-, k = 1.2 \times 10^6\ M^{-1}\ s^{-1} \quad (5)$$

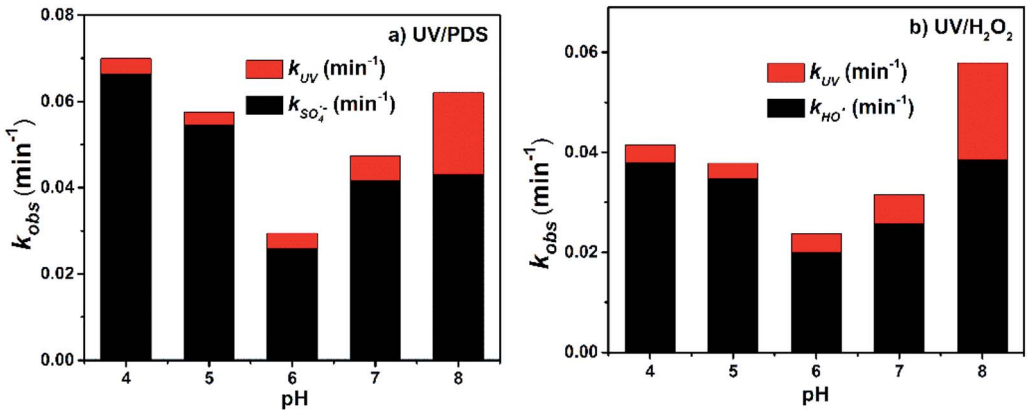

Fig. 2 Effects of pH on the degradation of 2-BP in UV/PDS and UV/H_2O_2 processes. Experimental conditions: [2-BP] = 10 μM; 10 mM phosphate buffer; [PDS] = [H_2O_2] = 0.5 mM.

$$HO^{\cdot} + H_2PO_4^{-} \rightarrow H_2O + HPO_4^{\cdot-},\ k = 2.0 \times 10^4\ M^{-1}\ s^{-1} \quad (6)$$

$$HO^{\cdot} + HPO_4^{2-} \rightarrow OH^{-} + HPO_4^{\cdot-},\ k = 1.5 \times 10^5\ M^{-1}\ s^{-1} \quad (7)$$

3.3. Effects of Cl^- on 2-BP degradation

The concentration of Cl^- ranges from 0.5 to 500 mM in different natural waters (*e.g.*, freshwater, surface water, groundwater and seawater),[32,33] and the influences of Cl^- (1, 5, 10, 100 and 500 mM) on the efficiency of 2-BP degradation in the UV/PDS and UV/H_2O_2 systems were investigated in this study.

As shown in Fig. 3, the degradation of 2-BP was inhibited when Cl^- increased from 1 mM to 100 mM in UV/PDS; however, when the concentration of Cl^- increased to 500 mM, the degradation rate of 2-BP was slightly enhanced. However, in the UV/H_2O_2 process, the presence of Cl^- always had a slight inhibitory effect on the degradation of 2-BP, and the inhibition degree almost did not vary with changing Cl^- concentration.

With changing Cl^- concentration, the direct photodegradation of 2-BP was almost unchanged; therefore, the variation of k_{obs} was mainly due to the effects of Cl^- on the oxidation of 2-BP by free radicals. When the concentration of Cl^- is low (≤10 mM), Cl^- will be converted by sulfate radical into $Cl^{\cdot}$ with weak capability of oxidizing 2-BP,[34] thus inhibiting the degradation of 2-BP (eqn (8)).[35,36] With further increase of the Cl^- concentration (≥100 mM), the Cl^- in the reaction system can be converted into HOCl with stronger oxidation through a series of reactions (eqn (9) to (12));[37] therefore, the degradation of 2-BP is enhanced.[38] In addition, compared with the UV/PDS process, the inhibition effects of Cl^- on the degradation of 2-BP are weak in the UV/H_2O_2 process. Because the reaction between $Cl^{\cdot}$ and $HO^{\cdot}$ is reversible, the addition of Cl^- has no significant effect on the concentration of $HO^{\cdot}$.

$$Cl^- + SO_4^{\cdot-} \rightarrow SO_4^{-} + Cl^{\cdot},\ k = 3.0 \times 10^8\ M^{-1}\ s^{-1} \quad (8)$$

$$Cl^- + Cl^{\cdot} \rightarrow Cl_2^{\cdot-},\ k = 8.5 \times 10^9\ M^{-1}\ s^{-1} \quad (9)$$

$$Cl_2^{\cdot-} + Cl_2^{\cdot-} \rightarrow Cl_2 + 2Cl^-,\ k = 9.0 \times 10^8\ M^{-1}\ s^{-1} \quad (10)$$

$$Cl_2^{\cdot-} + Cl^{\cdot} \rightarrow Cl_2 + Cl^-,\ k = 2.1 \times 10^9\ M^{-1}\ s^{-1} \quad (11)$$

$$Cl_2 + H_2O \rightarrow Cl^- + HOCl + H^+,\ k = 15\ M^{-1}\ s^{-1} \quad (12)$$

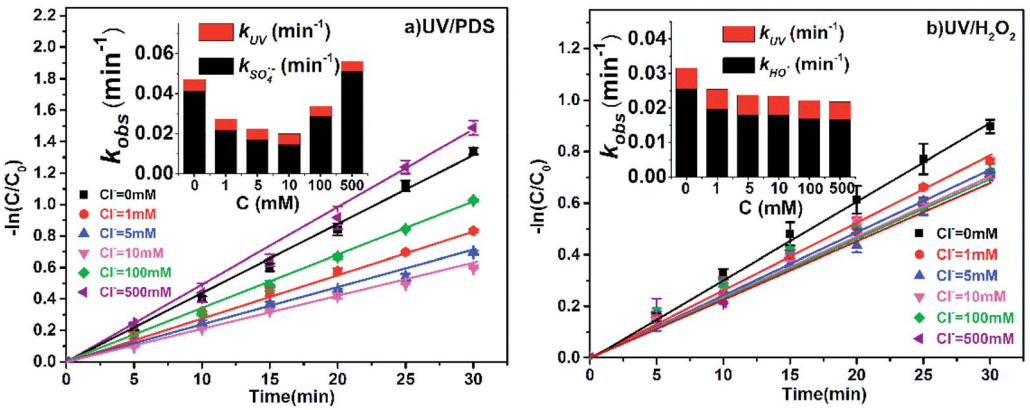

Fig. 3 Effects of Cl^- on the degradation of 2-BP in UV/PDS and UV/H_2O_2 processes. Experimental conditions: [2-BP] = 10 μM; 10 mM phosphate buffer (pH 7.0); [PDS] = [H_2O_2] = 0.5 mM.

3.4. Effects of HCO_3^- on the degradation of 2-BP

Bicarbonate is very common in natural water, with concentrations ranging from 0.4 to 4.4 mM.[33,39] The influence of HCO_3^- on the degradation efficiency of 2-BP in UV/PDS and UV/H_2O_2 was also explored (Fig. 4). The k_{obs} of 2-BP declined from 0.0264 to 0.0173 min^{-1} with increasing HCO_3^- concentration (1 mM to 5 mM) in the UV/PDS process and declined from 0.0206 to 0.0179 min^{-1} in the UV/H_2O_2 process. The presence of bicarbonate had little effect on the direct photodegradation of 2-BP; therefore, the main reason for the decrease of k_{obs} is the reduction of $k_{radicals}$ by bicarbonate.

It can be seen that the presence of HCO_3^- can effectively inhibit the degradation of 2-BP in both processes. This is because HCO_3^- can react with $SO_4^{\bullet-}$ and $HO^\bullet$ (eqn (13) and (14)) with high reaction rate constants (10^6 M^{-1} s^{-1}), and these reactions decrease the steady-state concentrations of $SO_4^{\bullet-}$ and $HO^\bullet$. In this process, although $CO_3^{\bullet-}$ was produced, the generated $CO_3^{\bullet-}$ reacted with the BPs with low reactivity.[18]

$$HCO_3^- + SO_4^{\bullet-} \rightarrow HSO_4^- + CO_3^{\bullet-},\ k = 9.1 \times 10^6\ M^{-1}\ s^{-1} \quad (13)$$

$$HCO_3^- + HO^\bullet \rightarrow H_2O + CO_3^{\bullet-},\ k = 8.5 \times 10^6\ M^{-1}\ s^{-1} \quad (14)$$

In addition, HCO_3^- suppressed the degradation of pollutants in the UV/PDS system more significantly. This is because the scavenging effect of HCO_3^- on $SO_4^{\bullet-}$ was stronger than that of $HO^\bullet$. By calculating the competitive kinetics, the ratio of $k_{OH^\bullet,HCO_3^-}/k_{OH^\bullet,BP}$ was found to be about 1.53 times higher than that of $k_{OH^\bullet,HCO_3^-}/k_{SO_4^{\bullet-},BP}$;[40,41] this indicates that HCO_3^- has a stronger scavenging effect on $SO_4^{\bullet-}$.

3.5. Effects of NOM on 2-BP degradation

The concentration of NOM in surface water is approximately 2.2 to 18 mgC L^{-1},[33,39] and the influence of NOM on 2-BP degradation was also investigated. As shown in Fig. 5, the k_{obs} of 2-BP in the UV/PDS and UV/H_2O_2 processes decreased from 0.0202 to 0.0136 min^{-1} and from 0.0202 to 0.0153 min^{-1}, respectively, with increasing addition of NOM (1 mgC L^{-1} to 10 mgC L^{-1}). Because NOM has a strong optical screening effect, the direct photodegradation rate of 2-BP was affected by NOM to some extent. It was found that with increasing NOM concentration, k_{UV} decreased gradually; simultaneously, $k_{radicals}$ also decreased significantly.

The existence of NOM can significantly inhibit the degradation of 2-BP in both processes. On the one hand, the inhibitory effect of NOM was attributed to light shielding because of the high molar absorption coefficient of NOM.[42] This light shielding effect of NOM reduced the photons absorbed by PDS and H_2O_2, resulting in decreases of the $SO_4^{\bullet-}$ and $HO^\bullet$ concentrations. On the other hand, it was previously reported that NOM can scavenge free radicals, leading to decreased $SO_4^{\bullet-}$ and $HO^\bullet$ concentrations. The reaction rate constants of NOM with $SO_4^{\bullet-}$ and $HO^\bullet$ were reported to be as high as 6.8×10^3 mgC L^{-1} s^{-1} and 1.4×10^4 mgC L^{-1} s^{-1}, respectively.[31,43]

3.6. Degradation products of 2-BP in UV/PDS and UV/H_2O_2 processes

The degradation products of 2-BP were detected by LC-MS/MS; the tentatively identified degradation products of 2-BP were ($[M - H]^{-1}$) 145.05, 109.03, 186.96, 292.95, 262.97, 338.87, 340.88, and 354.86. The products were further determined according to the identified values of the ($[M - H]^{-1}$) ratio and previous reports (Tables S7 and S8†). Here, ($[M - H]^{-1}$) 145.05, 292.96, 262.97, 338.87, and 340.88 were generated from the reaction of $SO_4^{\bullet-}$ with 2-BP. In comparison, ($[M - H]^{-1}$) 109.03, 186.96, 292.95, 262.97, 340.88, and 354.86 were produced from the reaction of $HO^\bullet$ with 2-BP. The different degradation products of $SO_4^{\bullet-}$ with 2-BP and $HO^\bullet$ with 2-BP can be attributed to their different mechanisms.

DFT was introduced to further analyze the transition state of 2-BP *via* calculating the HOMO orbital composition (Fig. S2†). According to the detected products and quantum chemical calculations, the reaction pathways were proposed (Fig. 6). C2, C5 and C4 in 2-BP were found to account for high percentages of the HOMO orbital composition, with 22.01%, 19.20% and 12.69%, respectively; this indicates that C2, C5 and C4 in 2-BP are most likely to be formed *via* electrophilic reactions. Thus, as

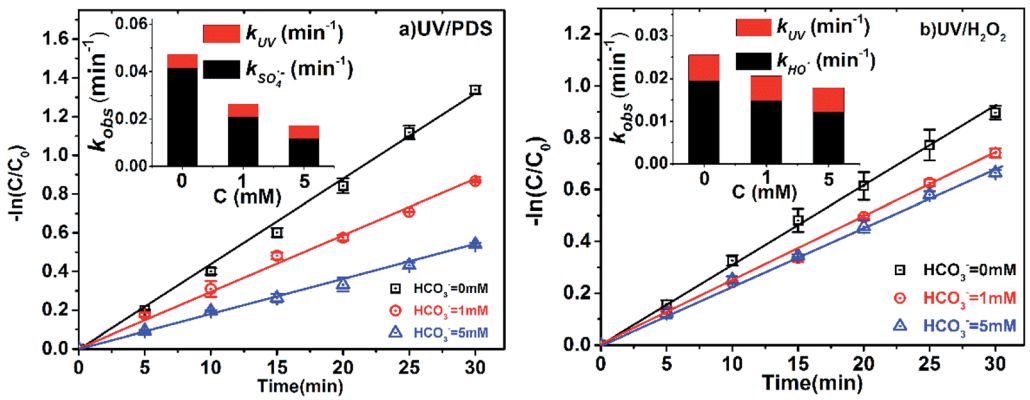

Fig. 4 Effects of HCO_3^- on the degradation of 2-BP in UV/PDS and UV/H_2O_2 processes. Experimental conditions: [2-BP] = 10 μM; 10 mM phosphate buffer (pH 7.0); [PDS] = [H_2O_2] = 0.5 mM.

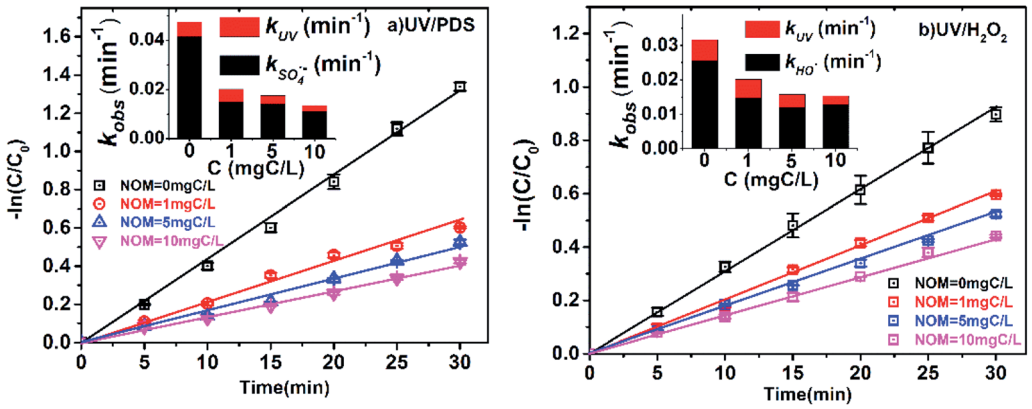

Fig. 5 Effects of NOM on the degradation of 2-BP in UV/PDS and UV/H_2O_2 processes. Experimental conditions: [2-BP] = 10 μM; 10 mM phosphate buffer (pH 7.0); [PDS] = [H_2O_2] = 0.5 mM.

the first step, $SO_4^{\bullet-}$ is most likely to attack C2 on the benzene ring and then produce the corresponding intermediates R_1, R_2 and R_3. The products of I, II and III were produced from the coupling of R_1, R_2 and R_3.[4] Then, these products (I, II and III) further reacted with $SO_4^{\bullet-}$, generating products IV and V; these may produce VII *via* a series of reaction processes, including ring-cleavage.

In comparison, the first step of the reaction of HO$^{\bullet}$ with 2-BP is different from that of the reaction of $SO_4^{\bullet-}$ with 2-BP based on the identified products. Bromohydroquinone (([M − H]$^{-1}$) 186.96) was the product derived from hydroxyl addition of 2-BP, and R_1 was further produced *via* elimination of one water molecule. In addition, catechol (([M − H]$^{-1}$) 109.03) was the product of the hydroxyl addition of R_3. The products I, II and III were also produced from the interactions of R_1, R_2 and R_3. ([M − H]$^{-1}$) 354.86 is the product formed from the reaction of HO$^{\bullet}$ with product I. The first steps of the product pathways further suggest that $SO_4^{\bullet-}$ is a strong one-electron oxidant that reacts with organic contaminants *via* electron transfer more readily than HO$^{\bullet}$.

Furthermore, variation of the TOC during degradation was monitored. The results showed that in the UV/PDS system, the mineralization rate of the pollutant was 33%, while the TOC value decreased slightly in the UV/H_2O_2 system (as shown in Fig. S3†); this indicates that more complete degradation occurred in the UV/PDS system. This can be attributed to the fact that more radicals can be formed in the UV/PDS process based on the higher molar extinction coefficient of PDS (*i.e.*, 21.1 M^{-1} cm^{-1}) than of H_2O_2 (*i.e.*, 18 M^{-1} cm^{-1}) and the higher quantum yield of $SO_4^{\bullet-}$ (*i.e.*, 0.7 mol per einstein) during UV photolysis of PDS than of HO$^{\bullet}$ (*i.e.*, 0.5 mol per einstein) during H_2O_2 photolysis.[34] It should be noted that the generation of toxic byproducts (such as hydroxylated polybrominated diphenyl ethers (OH-PBDEs) and hydroxylated polybrominated

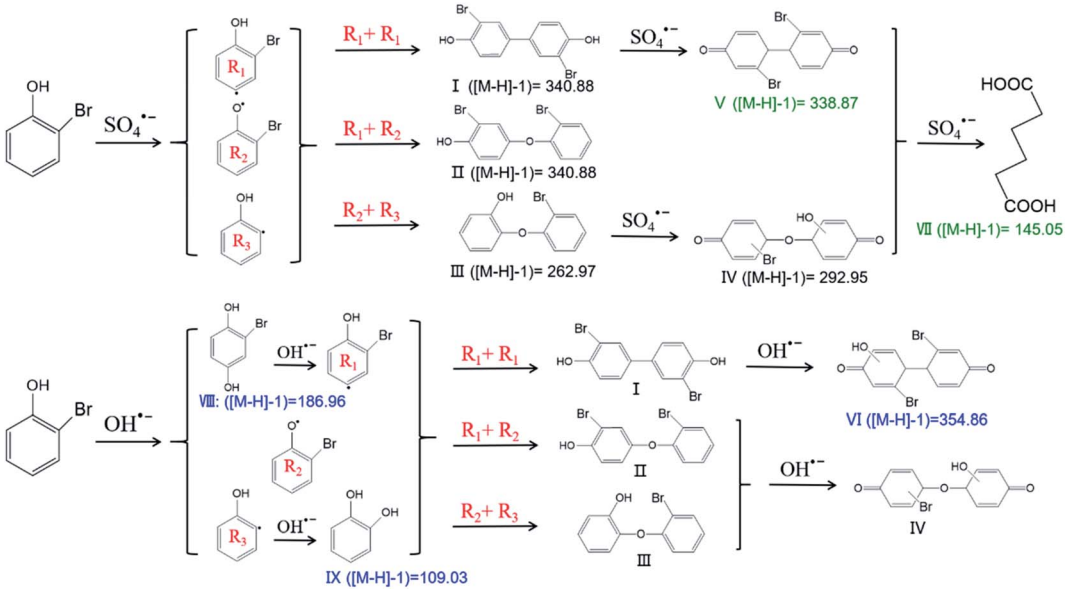

Fig. 6 The degradation products and pathways of 2-BP in UV/PDS and UV/H_2O_2 systems (R_1, R_2, R_3 are the predicted intermediates of 2-BP; I, II, III, IV, V, VI, VII are the identified products of 2-BP).

biphenyls (OH-PBBs)) in degradation processes should be of concern, given that high toxicity of these byproducts was reported in previous research.[18,34,44] Literature reports about the degradation of HPs showed that increasing the dosage of oxidant can not only effectively remove pollutants, but can also achieve better dehalogenation efficiencies.[3,34] It can also be inferred from the degradation of TOC that toxic byproducts can be gradually mineralized with increasing reaction time.

4. Conclusion

The degradation rates of HPs with different substitution positions in the UV/PDS process were in the order of *para*-substituted HPs (*i.e.*, 4-BP and 4-CP) > *ortho*-substituted HPs (*i.e.*, 2-BP and 2-CP) > *meta*-substituted HPs (*i.e.*, 3-BP and 3-CP), while in the UV/H_2O_2 process, the rates were in the order of *para*-substituted HPs > *meta*-substituted HPs > *ortho*-substituted HPs. The second-order reaction rate constant of $SO_4^{\bullet-}$ with substituted HPs was calculated to be (2.74 to 3.37) $\times$ 10^9 M^{-1} s^{-1}, and the second-order reaction rate constants between $HO^{\bullet}$ and the substituted HPs were (3.93 to 6.84) $\times$ 10^9 M^{-1} s^{-1}, respectively.

The presence of Cl^-, HCO_3^- and NOM could inhibit the degradation of 2-BP due to their ability of scavenging free radicals. The DFT calculations indicated that $SO_4^{\bullet-}$ reacts with HPs *via* electron transfer more readily than $HO^{\bullet}$. The products further confirmed that $SO_4^{\bullet-}$ is a strong one-electron oxidant that reacts with HPs mainly *via* electron transfer, while in the case of $HO^{\bullet}$, it reacts with HPs *via* electron transfer and hydroxyl addition.

Conflicts of interest

There are no conflicts to declare.

Acknowledgements

We gratefully acknowledge funding from the National Natural Science Foundation of China (No. 51608036, 51578066, and 41977317), Fundamental Research Funds for the Central Universities (No. 2015ZCQ-HJ-02), Natural Science Foundation of Beijing Municipality (No. 8182037), and Major Science and Technology Program for Water Pollution Control and Treatment (2017ZX07102-002).

References

1 C. Guan, J. Jiang, C. Luo, S. Pang, Y. Yang, Z. Wang, J. Ma, J. Yu and X. Zhao, *Chem. Eng. J.*, 2018, **337**, 40–50.
2 H. Zhao, J. Jiang, Y. Wang, H. Lehmler, G. R. Buettner, X. Quan and J. Chen, *Environ. Sci. Technol.*, 2015, **49**, 14120–14128.
3 B. Xie, X. Li, X. Huang, Z. Xu, W. Zhang and B. Pan, *J. Environ. Sci.*, 2017, **54**, 231–238.
4 K. Nomiyama, C. Kanbara, M. Ochiai, A. Eguchi, H. Mizukawa, T. Isobe, T. Matsuishi, T. K. Yamada and S. Tanabe, *Mar. Environ. Res.*, 2014, **93**, 15–22.
5 J. Jiang, Y. Gao, S. Y. Pang, Q. Wang, X. Huangfu, Y. Liu and J. Ma, *Environ. Sci. Technol.*, 2014, **48**, 10850–10858.
6 K. Lin, L. Song, S. Zhou, D. Chen and J. Gan, *Chemosphere*, 2016, **155**, 266–273.
7 C. Guan, J. Jiang, S. Pang, C. Luo, J. Ma, Y. Zhou and Y. Yang, *Environ. Sci. Technol.*, 2017, **51**, 10718–10728.
8 W. Sim, S. Lee, I. Lee, S. Choi and J. Oh, *Chemosphere*, 2009, **77**, 552–558.
9 C. M. Olsen, E. T. M. Meussen-Elholm, J. A. Holme and J. K. Hongslo, *Toxicol. Lett.*, 2002, **129**, 55–63.
10 E. Bruchajzer, J. A. Szymanska and J. K. Piotrowski, *Toxicol. Lett.*, 2002, **134**, 245–252.
11 Y. Dai, Y. Song, S. Wang and Y. Yuan, *Water Res.*, 2015, **71**, 64–73.
12 A. Meizler, F. Roddick and N. Porter, *Chem. Eng. J.*, 2011, **172**, 792–798.
13 F. Ghanbari, M. Moradi and F. Gohari, *Journal of Water Process Engineering*, 2016, **9**, 22–28.
14 G. Matafonova and V. Batoev, *Water Res.*, 2018, **132**, 177–189.
15 E. Simonenko, A. Gomonov, N. Rolle and L. Molodkina, *Procedia Eng.*, 2015, **117**, 337–344.
16 P. Avetta, A. Pensato, M. Minella, M. Malandrino, V. Maurino and C. Minero, *Environ. Sci. Technol.*, 2015, **49**, 1043–1050.
17 M. W. Lam and S. A. Mabury, *Aquat. Sci.*, 2005, **67**, 177–188.
18 C. Luo, J. Gao, D. Wu, J. Jiang, Y. Liu, W. Zhou and J. Ma, *Chem. Eng. J.*, 2019, **358**, 1342–1350.
19 L. Xu, R. Yuan, Y. Guo, D. Xiao, Y. Cao, Z. Wang and J. Liu, *Chem. Eng. J.*, 2013, **217**, 169–173.
20 T. K. Lau, W. Chu and N. J. D. Graham, *Environ. Sci. Technol.*, 2007, **41**, 613–619.
21 H. V. Lutze, S. Bircher, I. Rapp, N. Kerlin, R. Bakkour, M. Geisler, C. V. Sonntag and T. C. Schmidt, *Environ. Sci. Technol.*, 2015, **49**, 1673–1680.
22 M. Ahmadi, S. Samarbaf, M. Golshan, S. Jorfi and B. Ramavandi, *Data in Brief*, 2018, **20**, 582–586.
23 R. O. Rahn, M. I. Stefan, J. R. Bolton, E. n. M. Goren, P. S. Shaw and K. R. Lykke, *Photochem. Photobiol.*, 2003, **78**, 146–152.
24 T. Lu and F. Chen, *J. Comput. Chem.*, 2012, **33**, 580–592.
25 K. Mangalgiri and L. Blaney, *Environ. Sci. Technol.*, 2017, **51**, 12310–12319.
26 P. Sun, C. Tyree and C. Huang, *Environ. Sci. Technol.*, 2016, **50**, 4448–4458.
27 P. Xie, J. Ma, W. Liu, J. Zou, S. Yue, X. Li, M. R. Wiesner and J. Fang, *Water Res.*, 2015, **69**, 223–233.
28 Z. Yang, R. Su, S. Luo, R. Spinney, M. Cai, R. Xiao and Z. Wei, *Sci. Total Environ.*, 2017, **590**, 751–760.
29 S. Luo, L. Gao, Z. Wei, R. Spinney, D. D. Dionysiou, W. Hu, L. Chai and R. Xiao, *Water Res.*, 2018, **137**, 233–241.
30 J. Jiang, H. Zhao, S. Liu, X. Chen, X. Jiang, J. Chen and X. Quan, *J. Photochem. Photobiol., A*, 2017, **336**, 63–68.
31 F. Wang, W. Wang, S. Yuan, W. Wang and Z. Hu, *J. Photochem. Photobiol., A*, 2017, **348**, 79–88.
32 M. Sturini, A. Speltini, F. Maraschi, A. Profumo, L. Pretali, E. Fasani and A. Albini, *Environ. Sci. Technol.*, 2010, **44**, 4564–4569.

33 C. Zhou, J. Chen, Q. Xie, X. Wei, Y. Zhang and Z. Fu, *Chemosphere*, 2015, **138**, 792–797.
34 C. Luo, J. Jiang, J. Ma, S. Pang, Y. Liu, Y. Song, C. Guan, J. Li, Y. Jin and D. Wu, *Water Res.*, 2016, **96**, 12–21.
35 R. Zhang, P. Sun, T. H. Boyer, L. Zhao and C. Huang, *Environ. Sci. Technol.*, 2015, **49**, 3056–3066.
36 K. Yin, Y. Deng, C. Liu, Q. He, Y. Wei, S. Chen, T. Liu and S. Luo, *Chem. Eng. J.*, 2018, **346**, 298–306.
37 Y. Yang, J. Pignatello, J. Ma and W. Mitch, *Environ. Sci. Technol.*, 2014, **48**, 2344–2351.
38 Z. Wang, R. Yuan, Y. Guo, L. Xu and J. Liu, *J. Hazard. Mater.*, 2011, **190**, 1083–1087.
39 A. Lin, X. Wang and W. Lee, *Environ. Sci. Technol.*, 2013, **47**, 4104–4112.
40 M. Kwon, S. Kim, Y. Yoon, Y. Jung, T. Hwang, J. Lee and J. Kang, *Chem. Eng. J.*, 2015, **269**, 379–390.
41 X. Liu, L. Fang, Y. Zhou, T. Zhang and Y. Shao, *Environ. Sci. Technol.*, 2013, **37**, 4790–4797.
42 D. Vione, D. Fabbri, M. Minella and S. Canonica, *Water Res.*, 2018, **128**, 38–48.
43 Y. Ahn, D. Lee, M. Kwon, I. Choi, S. Nam and J. Kang, *Chemosphere*, 2017, **184**, 960–968.
44 K. Lin, C. Yan and J. Gan, *Environ. Sci. Technol.*, 2014, **48**(1), 263–271.

